

Structure and Magnetic Characterization of Core-Shell Fe@ZrO₂ Nanoparticles Synthesized by Sol-Gel Process

Girija S. Chaubey and Jinkwon Kim*

Department of Chemistry, Kongju National University, Kongju, Chungnam 314-701, Korea. *E-mail: jkim@kongju.ac.kr

Received June 27, 2007

Highly crystalline, uniform Fe nanoparticles were successfully synthesized and encapsulated in zirconia shell using sol-gel process. Two different approaches have been employed for the coating of Fe nanoparticle with zirconia. The thickness of zirconia shell can be readily controlled by altering molar ratio of Fe nanoparticle core to zirconia precursor in the first case where as reaction time was found to be most effective parameter to controlled the shell thickness in the second method. The structure and magnetic properties of the ZrO₂-coated Fe nanoparticles were studied. TEM and IIRTEM images show a typical core/shell structure in which spherical α -iron crystal sized of ~25 nm is surrounded by amorphous ZrO₂ coating layer. TGA study showed an evidence of weight loss of less than 2% over the temperature range of 50-500 °C. The nanoparticles are basically in ferromagnetic state and their magnetic properties depend strongly on annealing temperature. The thermal treatment carried out in as-prepared sample resulted in reduction of coercivity and an increase in saturation magnetization. X-ray diffraction experiments on the samples after annealing at 400-600 °C indicate that the size of the Fe@ZrO₂ particles is increased slightly with increasing annealing temperature, indicating the ZrO₂ coating layer is effective to interrupt growing of iron particle according to heat treatment.

Key Words : Iron nanoparticles, Core-shell, Zirconium oxide, Coating, Magnetization

Introduction

The recent advances to achieve nanoscale particles stem from their fundamental and technological importance.¹⁻⁴ Nanoparticles exhibit very interesting electrical, optical and magnetic properties which are distinct from their bulk counterparts. As nanoparticles become smaller they become more air sensitive. In particular, Fe nanoparticles are susceptible to rapid oxidation to the extent of pyrophoricity. The pure magnetic particles tend to form large aggregates and their original structure may get changed if they are not stable enough, resulting in the alternation of magnetic properties. One way to overcome these drawbacks is to coat the particles with protective layer prior to being used. For example, in clinical applications the nanoparticles should be protected from leaching in an acidic environment.^{5,6}

Although a considerable amount of research involving the passivation of the magnetic nanoparticles of Fe, Co, and Ni by another layer such as SiO₂ and polymers has been conducted,⁷⁻¹² there has been a large interest for technical development to get uniform-size metal nanoparticles coated by thin layer of highly insulating materials. Especially, as electronic devices become smaller, soft magnet materials showing high permeability even at high frequency are to be essential. However, conventional soft magnetic materials based on alloys do not working above 1 MHz mainly due to Eddy current losses. To reduce Eddy current losses, a material should have high resistivity, in addition to high induction and high permeability. One method for creating such a material is to create metal-ceramic nano composite in which nanometer-sized magnetic domains are separated by thin insulating layers to increase electric resistivity of metal

based soft magnetic materials.¹³ ZrO₂ was selected as a coating layer, because it is not only good insulating property but also has other merits for powder compacting process, such as chemical inertness, wear resistance and high fracture toughness, etc. The core Fe particle should be crystalline to get high saturation magnetization. Prompted by this hypothesis, we have synthesized highly crystalline spherical Fe nanoparticles coated uniformly by ZrO₂ thin layer. Structural, thermal, and magnetic properties of Fe@ZrO₂ have been investigated.

Experimental

The synthesis was performed under nitrogen atmosphere using standard Schlenk techniques. Iron(III) chloride hexahydrate (98%), sodium borohydride powder (98%) and zirconium(IV) tert-butoxide were obtained from Aldrich Chemical Co. and used as received. Distilled water was purged with nitrogen for several hours prior to use. The synthesis route for iron nanoparticle is slightly modified from the method reported earlier.¹⁴ To a three necked round bottom flask, 16.06 mmol of sodium borohydride was dissolved in 50 mL of degassed water and stirred mechanically for 30 minutes under nitrogen. To this mixture, a freshly prepared 1.75 mmol of FeCl₃·6H₂O dissolved in 50 mL of degassed water was injected under vigorous stirring. A black color solution was produced with vigorous evolution of gas which continues for 15 minutes. The resulting black powder was further aged for 30-45 minutes. The excessive use of borohydride was a key factor for the rapid and uniform growth of iron particles. The metal particles formed from the above reaction were washed with large volume of water for

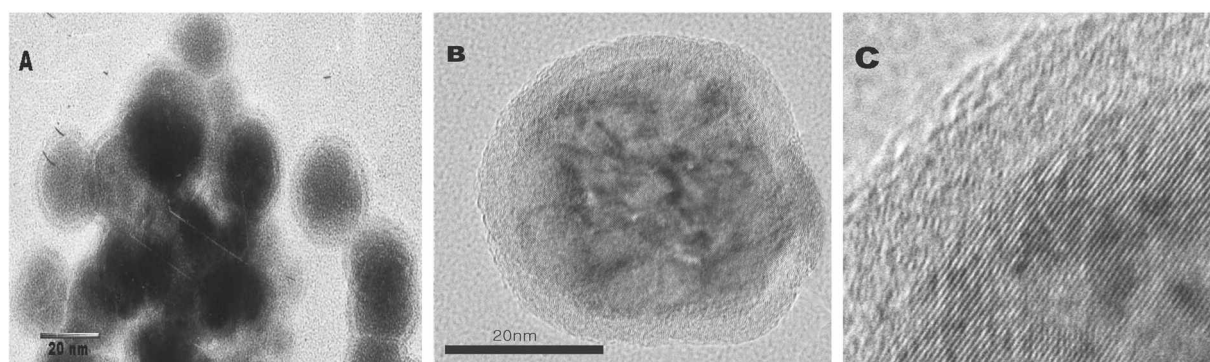


Figure 1. (A) TEM image of ZrO_2 coated Fe nanoparticles for the sample RT. (B) HRTEM image of a single core-shell nanoparticle of sample RT. The dark core is α -iron and the light shell is ZrO_2 . (C) High magnification view of Fe@ZrO_2 nanoparticle showing the lattice fringes of the core and amorphous nature of the shell.

at least three times and dry *in vacuo*. Then, Fe nanoparticles were encapsulated in zirconia.

Two different approaches have been employed to generate zirconia coating on the surface of iron nanoparticles. Our first method was based on base catalyzed hydrolysis and condensation, in brief, Fe nanoparticle core and zirconium (IV) tert-butoxide in the molar ratio 20:1 was taken in inert atmosphere. 50 mL of ethanol was added and the reaction mixture stirred mechanically. Under vigorous stirring condition, 1 mL NH_4OH (30%) was injected with a syringe and the reaction mixture was continued to stirred rigorously under nitrogen for 4 hours. The encapsulated particles were isolated by centrifugation (10000 rpm for 5 min) and residual zirconia formed during hydrolysis-condensation was removed by washing several times with ethanol. Keeping other conditions identical, the thickness of zirconia shell could be controlled by simply changing the molar ratios of Fe nanoparticle core to zirconia precursor.

The second approach was relied on uncatalyzed coating of iron nanoparticle through hydrolysis and condensation. The procedure is as follows: 0.3 g of Fe nanoparticles core and 0.1 mL of zirconium(IV) tert-butoxide was taken in inert atmosphere. 50 mL of ethanol was added to it and the reaction mixture was stirred mechanically in air. The zirconia coated Fe nanoparticles were separated and washed *via* centrifugation by above mentioned procedure. The thickness of zirconia shell could be controlled by stopping the reaction at different intervals of time.

X-ray diffraction (XRD) measurements were carried out on a Rigaku, AX-2500 diffractometer ($\text{Cu K}\alpha$ radiation = 1.54 Å) at 40 kV and 150 mA. Fe@ZrO_2 nanoparticles were characterized by a JEOL 2000EX and a JEOL 4010 transmission electron microscope. The TEM samples were prepared by placing 10-15 drops of acetone dispersed nanoparticles solution onto a carbon-coated copper TEM grid, which was left to dry in air. The thermal gravimetric analysis (TGA) was obtained using a SETRAM 92-18 instrument under a atmosphere of argon using heating rate 10 °C/min. Heat treatments to anneal the samples were carried out in quartz tube under H_2 over a temperature range of 400-600 °C. The magnetic properties were studied using a Quantum Design MPMS-5S SQUID magnetometer.

Results and Discussion

Our primary effort was focused on synthesis and coating of iron nanoparticles with dimensions in the range of 20-30 nm. The black iron powder obtained by the method reported earlier¹⁴ was amorphous in nature. Our modified synthetic procedure has the potential to induce crystalline character on the sample which can be recognized from the high intensity XRD reflection peaks of the sample without heat treatment. The core/shell structure of the particle was characterized by TEM. As shown in Figure 1A, the nanoparticles appear almost spherical and tend to form chains, indicating ferromagnetic interaction. An aggregation between iron nanoparticles prior to or during coating process sometimes led to the trapping of multiple nuclei in a single zirconia shell. The particle consists of metallic cores having average diameter of 25 nm, surrounded by a ZrO_2 shell, averaging 2.5 nm in thickness, for a total average diameter of 30 nm. Detailed structure of a single Fe@ZrO_2 particle is characterized with HRTEM, as shown in Figure 1B. The lattice fringes of the core are clearly shown in the image. The image shows the ZrO_2 shell is amorphous. Clearly visible lattice fringes on dark core region of the high magnified view of core-shell nanoparticles provide an addition evidence for crystalline nature of the iron nanoparticle (Figure 1C).

Two different approaches have been applied to generate zirconia coating on the surface of iron nanoparticles. While both the methods based on well known Stöber process, the first one was ammonia catalyzed coating of iron nanoparticles through hydrolysis and condensation of a sol-gel precursor under inert atmosphere. The other method was consisting of almost similar effort except no ammonia catalyst is applied in this case and the reaction was carried out in open air. Owing to the highly reactive characteristics of iron nanoparticle surface, it bears an oxide layer. It is plausible that this oxide layer facilitates the covalent binding of the zirconia to the metal surface.

Several parameters such as the growth time, the concentration of ammonia catalyst, could be responsible for the thickness of the zirconia shell, we observed that the most convenient way to adjust shell thickness is by changing the molar ratio of iron nanoparticle core to zirconia precursor in

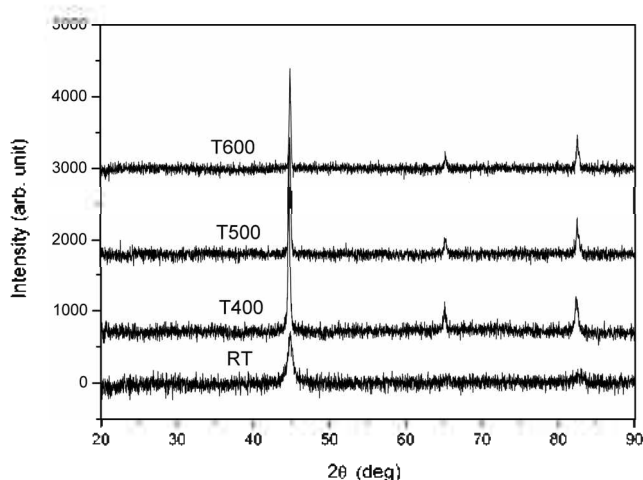


Figure 2. X-ray diffraction patterns for the samples RT, T400, T500, T600.

former method. For example, for the molar ratio 20:1 of iron nanoparticle core to zirconium (IV) tert-butoxide, a zirconia shell of an average thickness 2.4 nm is obtained over iron nanoparticles where as for molar ratio 10:1 of the same precursors, a zirconia shell of mean thickness 2.9 nm is obtained over Fe nanoparticles. In latter method, the reaction time was found to be the most effective and reproducible way to control the shell thickness. For the molar ratio 20:1 of iron nanoparticle core to zirconia precursor, a mean shell thickness of 2.5 nm was obtained after 24 hours of reaction where as an average 3 nm zirconia shell was observed after 48 hours of reaction. However, we did not observe any major difference in magnetic properties of the zirconia coated Fe nanoparticles synthesized by both methods. The magnetic properties presented in this paper were studies on 25 nm of Fe nanoparticles coated with 2.5 nm zirconia shell, synthesized by second method.

The thermal behavior of the initial particles was studied by TGA. In the temperature range between 50 to 500 °C, TGA showed a weight lose of less than 2%, which can be associated with the release of adsorbed water and alcohols. The particles were annealed at three different temperature (400, 500, 600 °C) for one hour under hydrogen. The XRD patterns of the four nanoparticle samples are shown in Figure 2. All of the diffraction patterns of four samples match up to only bcc Fe structure and shows no peak for Fe-oxide or crystalline ZrO₂. From the line width of the main peak around 44.6°, the mean size of the Fe particles was estimated according to the Scherrer formula. The mean particle size calculated using Scherrer equation is close to that observed in TEM image (Figure 1A). The results are summarized in Table 1. It is evident that the particle size increases slightly with increase in annealing temperature, indicating the ZrO₂ shell interrupts effectively growing of Fe crystals.

Figure 3 shows the corresponding changes in magnetization curves of the as-prepared and the annealed samples. High saturation magnetization is desirable for most applications. The specific saturation magnetizations at 5 K are

Table 1. Change of particle size, saturation magnetization and coercivity according to heat treatment

Sample ^a	Annealing temperature [°C]	Particle size [nm]	Coercivity at 300 K [Oe]	Saturation magnetization at 5 K [emu/g]
RT	—	25 ^b	420	150
T400	400	30.7 ^c	160	172
T500	500	33.1 ^c	138	190
T600	600	37.3 ^c	32	206

^aRT represents the nanoparticle sample synthesized at room temperature. T400, T500, T600 represent the samples of nanoparticle annealed at 400, 500 and 600 °C, respectively. ^bThe particle size estimated from TEM and ^cthe particle size estimated from the powder X-ray diffraction peak.

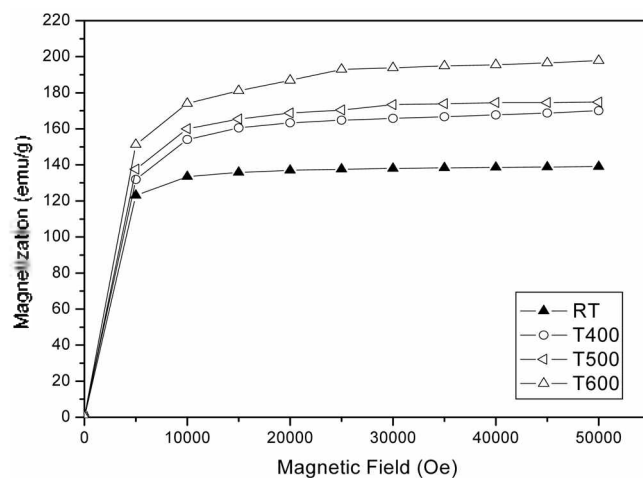


Figure 3. Magnetization vs. magnetic field measured at 300 K for the samples RT, T400, T500 and T600.

summarized in Table 1. The estimated saturation magnetization (M_s) is around 139 emu/g for as-prepared sample at 300 K (~150 emu/g at 5 K). For comparison, the standard crystalline bcc Fe has M_s ~222 emu/g at 298 K¹⁵ and the value of bulk amorphous Fe is around 156 emu/g.¹⁶ In addition, the saturation magnetization was found to increase with increasing annealing temperature of the samples. A similar behavior for magnetization was observed in Fe@SiO₂ nanoparticle.¹⁷

The temperature dependence of zero-field-cooled magnetization (ZFCM) and field cooled magnetization (FCM) for RT sample was measured in an applied magnetic field of 100 Oe between 5 K and 300 K. The result shows an irreversible magnetization-temperature behavior and no superparamagnetic relaxation behavior, indicating the particles are basically in the ferromagnetic state.

Magnetic hysteresis curves for the samples RT and T600 at 300 K are shown in Figure 4. The coercivity for the sample RT at 300 K was 420 Oe whereas for the sample T600, it was observed to be 32 Oe. The coercivity was found to depend strongly on particle size.¹⁸ For Fe nanoparticles, maximum coercivity is found at around 20 nm. An increase in particle size was observed with increase in annealing temperature which account for the significant decrease in coercivity.

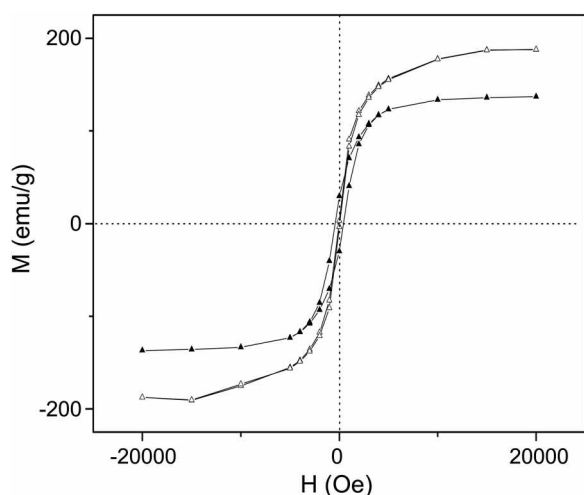


Figure 4. Hysteresis loops for samples RT (▲) and T600 (△) at 300 K.

Conclusions

The synthetic procedure presented here represents a substantial step forward in the ability to synthesize highly crystalline, uniform Fe nanoparticles encapsulated in zirconia shell using sol-gel process. The zirconia coating protects the magnetic particles from possible oxidation in surrounding environment, prevents them from further aggregation, and reduces interparticle magnetic interaction retaining the magnetic properties of each particle intact. The nanoparticles are basically in ferromagnetic state and their magnetic properties depend strongly on annealing temperature. The particles treated at higher temperature exhibit higher saturated magnetization and lower coercivity. Consolidation experiments of these particles for application to soft magnet are under investigation.

Acknowledgements. This work has been supported by the SRC/ERC program (Grant No. R11-2005-048-00000-0) of MOST/KOSEF.

References

- Bradley, J. S. *Cluster and Colloids*; Schmid, G., Ed.; VCH: 1994.
- (a) Murray, C. B.; Kagan, C. R.; Bawendi, M. G. *Science* **2000**, *287*, 1989. (b) Jun, Y.; Jang, J.; Cheon, J. *Bull. Korean Chem. Soc.* **2006**, *27*, 965.
- (a) Alivisatos, A. P. *Science* **1996**, *271*, 933. (b) Caruso, F. *Adv. Mater.* **2001**, *13*, 11.
- (a) Liz-Marzan, L. M.; Giersig, M.; Mulvaney, P. *Chem. Commun.* **1996**, 731. (b) Liz-Marzan, L. M.; Giersig, M.; Mulvaney, P. *Langmuir* **1996**, *12*, 4329.
- Liu, Q.; Xu, Z.; Finch, J. A.; Egerton, R. *Chem. Mater.* **1998**, *10*, 3936.
- Olsvik, O.; Popovic, T.; Skjerve, E.; Cudjoe, K. S.; Horns, E.; Ugelstad, J.; Uhl, M. *Clin. Microbiol. Rev.* **1994**, *7*, 43.
- Wu, M.; Yang, Y. D.; Hui, S.; Xiao, T. D.; Ge, S.; Hines, W. A.; Budnick, J. I. *J. Appl. Phys.* **2002**, *92*, 491.
- Pathmanoharan, C.; Philipse, A. P. *J. Colloid Interface Sci.* **1998**, *205*, 340.
- Klotz, M.; Ayrat, A.; Guizard, C.; Menager, C.; Cabuil, V. *J. Colloid Interface Sci.* **1999**, *220*, 357.
- Szabo, D. V.; Vollath, D. *Adv. Mater.* **1999**, *11*, 1313.
- Ennas, E.; Mei, A.; Musinu, A.; Piccaluga, G.; Pinna, G.; Solinas, S. *J. Non-Cryst. Solids* **1998**, *232-234*, 587.
- Tartaj, P.; Serna, C. J. *J. Am. Chem. Soc.* **2003**, *125*, 15754.
- Bas, J. A.; Caleo, J. A.; Dougan, M. J. *J. Magn. Magn. Mater.* **2003**, *254-255*, 391.
- Glavee, G. N.; Klabunde, K. J.; Sorensen, C. M.; Hadjipanayis, G. C. *Inorg. Chem.* **1995**, *9*, 28.
- Cullity, B. D. *Introduction to Magnetic Materials*; Addison-Wesley: 1972.
- Suslick, K. S.; Fang, M.; Hyeon, T. *J. Am. Chem. Soc.* **1996**, *118*, 11960 and references cited therein.
- Wu, M.; Yang, Y. D.; Hui, S.; Xiao, T. D.; Ge, S.; Hines, W. A.; Budnick, J. I.; Yacaman, M. J. *J. Appl. Phys.* **2002**, *92*, 6809.
- (a) Chen, C.; Kitakami, O.; Shimada, Y. *J. Appl. Phys.* **1998**, *84*, 2181. (b) Gangopadhyay, S.; Hadjipanayis, G. C.; Dale, B.; Sorensen, C. M.; Klabunde, K. J.; Papaefthymiou, V.; Kostika, A. *Phys. Rev.* **1992**, *B45*, 9778. (c) Zhao, S.-Y.; Lee, D. K.; Kim, C. W.; Cha, H. G.; Kim, Y. H.; Kang, Y. S. *Bull. Korean Chem. Soc.* **2006**, *27*, 237.